http://www.esajournals.org/doi/pdf/10.1890/14-1528.1

ECOLOGICAL
SOCIETY
OF AMERICA

Ecology/Ecological Monographs/Ecological Applications

Landscape Fragmentation, Severe Drought and the New Amazon Forest Fire Regime

Ane A. Alencar[1], Paulo M. Brando[1,2], Gregory P. Asner[2], Francis E. Putz[3]

[1]Instituto de Pesquisa Ambiental da Amazônia, SHIN CA5 J2 Sala 309, Brasilia DF 71503-505 Brazil; E-mail: ane@ipam.org.br

[2]Department of Global Ecology, Carnegie Institution for Science, 260 Panama Street, Stanford CA 94305 USA; E-mail: pbrando@carnegiescience.edu; gpa@carnegiescience.edu

[3] Department of Biology, University of Florida, Gainesville, FL 32641-8526 USA; E-mail: fep@ufl.edu

Abstract

Changes in weather and land use are transforming the spatial and temporal characteristics of fire regimes in Amazonia, with important effects on the functioning of dense (i.e., closed canopy), open canopy, and transitional forests across the Basin. To quantify, document and describe the characteristics and recent changes in forest fire regimes, we sampled 6 million ha of these three representative forests of the eastern and southern edges of the Amazon using 24 years (1983-2007) of satellite-derived annual forest fire scar maps and 16 years of monthly hot pixel information (1992-2007). Our results reveal that changes in forest fire regime properties differentially affected these three forest types in terms of area burned and fire scar size, frequency and seasonality. During the study period, forest fires burned 15% (0.3 million ha), 44% (1 million ha) and 46% (0.6 million ha) of dense, open, and transitional forests, respectively. Total forest area burned and fire scar size tended to increase over time (even in years of average rainfall in open canopy and transitional forests). In dense forests, most of the temporal variability in fire regime properties was linked to ENSO-related droughts. Compared with dense forests, transitional and open forests experienced fires twice as frequently, with at least 20% of these forests' areas burning two or more times during the 24-year study period. Open and transitional forests also experienced higher deforestation rates than dense forests. During drier years, the end of the dry season was delayed by about a month, which resulted in larger burn scars and increases in overall area burned later in the season. These observations suggest that climate-mediated forest flammability is enhanced by landscape fragmentation caused by deforestation, as observed for open and transitional forests in the Eastern portion of the Amazon Basin.

Keywords: fire regime, forest fires, fire frequency, fire interval, fire size, seasonality, fire history, ENSO, Amazon, land use change, climate change, forest fragmentation

Introduction

Pre-Columbian fire return intervals in Amazonian forests reportedly ranged from 400 to 1,000 years (Thonicke et al. 2001) and occurred mostly during rare droughts caused by Mega El Nino Southern Oscillation - ENSO (Sanford et al. 1985, Meggers 1994, Bush et al. 2008). In contrast, forest fires in Amazonia are now common due to fundamental changes in the region’s weather and landscape (Alencar et al. 2004, Cochrane and Laurance 2008, Morton et al. 2013). During recent decades, for example, both ENSO and Atlantic Multi-Decadal Oscillation (AMO) events caused widespread droughts (Yoon and Zeng 2010, Chen et al. 2011, Marengo et al. 2011), while people cleared, fragmented, and degraded large tracts (Asner et al. 2005a, Fearnside 2005, Broadbent et al. 2008, Souza et al. 2013). Together, these droughts and human-related activities were associated with large forest fires (Alencar et al. 2006, Morton et al. 2013). Understanding past and current variability in Amazonian fire regimes in different forest types is central to predicting future fire frequencies, burn areas, intensities, seasonality, and severity. If climate change and increased forest degradation continue, fires may burn more frequently and expand to larger areas, perhaps including landscapes that otherwise are fire resistant.

Deforestation influences Amazonian fire regimes because it results in increased sources of ignition, increased forest edge lengths, and alterations of regional climates (Cochrane and Laurance 2002, Aragão et al. 2008, Da Silva et al. 2008). It is therefore no surprise that ~85,000 km2 of primary forest burned along the ‘Arc of Deforestation’ during the 2000s (2000 – 2009), while a much larger area became flammable (Nepstad et al. 2004, Lewis et al. 2011). Given this logical interpretation of the events, it is surprising that forest fire activity continued to increase in the years after 2005 as deforestation rates decreased (Aragão and Shimabukuro 2010, Alencar et al. 2011). Researchers attributed high fire activity in 2005, 2007, and 2010 to dry and warm climatic conditions (Aragão et al. 2007, Zeng et al. 2008, Chen et al. 2011, Marengo et al. 2013), but the underlying mechanisms driving this process remain unclear. There is still a gap in understanding recent spatial and temporal changes in Amazonian forest fire regime properties, as well as how these properties have changed over time and among forest types.

One of the challenges in tropical fire ecology is in quantifying changes in fire regime properties based on an integrated set of metrics that are spatially-explicit and that cover long time-periods. Amazonian forest fire detection and quantification usually relies on coarse products that cannot properly map small forest fires (Morton et al. 2011). Moreover, these time series studies mostly began only in the early 2000s, which makes it difficult to identify trends in fire activity and to integrate changes in fire regimes with weather and land cover change (Morton et al. 2013). Integrated assessments of fire activity that are based on several fire metrics are also rare, and most studies tend to combine different Amazonian forest types with substantially different flammability (Alencar et al. 2006, Alencar et al. 2011, Morton et al. 2013).

We analyze a suite of critically important fire regime properties in Amazonia (i.e., fire extent, patch size, frequency, and seasonality) and the effects of some of these properties on the canopy cover of dense (i.e., closed canopy), open canopy, and transitional forests. We assess how changes in the fire regime vary among these three common forest types, and consider how they have evolved over a 24-yr time period (1983 to 2007). We use three forest type regions delimited by NASA Landsat satellite scenes to derive high-resolution burn scar maps (Alencar et al. 2011). We also assess changes in fire seasonality based on measures of monthly hot pixel detections of ignition sources for forest fires for a 16-yr time series (1992 - 2007) with Advanced Very High Resolution Radiometer (AVHRR) data on board of NOAA Satellite for the same forest regions. These elements of the fire regime provide information that can be used to estimate probabilities of forest fires and may help to predict the future of

Amazonian forest fires in response to deforestation, forest degradation, and increasingly frequent, prolonged, and intense droughts.

Materials and Methods

Study regions

Our study focuses on a corridor of deforestation in dense (i.e., closed canopy), open canopy, and transitional forests in eastern Amazon (Figure 1). These three vegetation types differ in structure and composition (RADAMBRASIL 1981). While dense forest has abundant trees 25-35 m tall, open canopy forest has only scattered emergent trees of about the same height. Transitional forest is shorter (15-25 m) than open forest, but has a more homogeneous closed canopy. The average aboveground biomass of these three vegetation types are 350, 250, and 200 Mg ha^{-1} for dense, open, and transitional forests, respectively (Baccini et al. 2012).

The dense, open, and transitional forests are represented by regions of 180x180 km delimited by the Landsat scenes path and row 223/62, 224/66 and 224/68 respectively, located along a precipitation gradient but experiencing similar influences of dry-air inputs during the dry season (Davidson et al. 2012). While the dense forest region receives an average annual rainfall of 2,200 mm, the open and transitional forests receive only 1,700 mm and 1,300 mm, respectively. The dry season (rainfall < 100 mm/month) in the whole region runs from June to November but peaks in September-October in the dense forest, and August-September in the open and transitional forest regions (Villar et al. 2009). Soils under these forest types are predominantly yellow latosols in dense forest, spodozols in open forest, and a mixture of red-yellow latosols and spodozols in the transitional forest (RADAMBRASIL 1981).

The study forest regions have experienced extensive deforestation and land use change, mainly for cattle ranching, with slash-and-burn agriculture near the settlements (Fearnside 2005, Pacheco 2009, Bowman et al. 2012). Logging is still a major economic activity, particularly in the dense forests (Asner et al. 2005a, Merry et al. 2009), with fewer species being harvested from the open and transitional forests (Lentini et al. 2005). Large-scale mechanized farming of soybeans, rice and corn are underway in the region, mainly in what was transitional forest (Macedo et al. 2012). Collectively these processes have resulted in landscape mosaics in which 71%, 45% and 50% of the original dense, open canopy, and transitional forests, respectively, remain standing (Table 1).

Mapping forest fires and fire ignition sources

To map annual forest fires in the three forest regions, we used 72 multispectral mid-resolution satellite images from Landsat 5 Thematic Mapper (TM) and Landsat 7 Enhanced Thematic Mapper Plus (ETM+). These covered a time series from 1983 to 2007 mapped on images from 1984 to 2008. Only images from early dry season (May to July) were used, so as to avoid double counting of fires in the same year or misrepresenting the year that a fire actually occurred, always accounting for fires that occurred in the previous calendar year. Once the images were radiometrically calibrated, converted to reflectance, co-registered, and geo-rectified (description in (Asner et al. 2005b)), we classified them into burned or non-burned based on the CLAS-BURN spectral unmixing routine and the Burn Scar Index algorithm. CLAS-Burn was developed to map only fire scars that burned within the previous 12 months, while the unburned class includes never-burned forest plus burned sites that have been recovering for at least two years since the last burn. This routine and algorithm (described in the detail in Alencar et al. (2011) accurately classified 89%, 79%, and 88% of the landscape burn scars from 2006 and 2007 that were visited in the field in the dense, open, and transitional forest study regions, respectively. CLAS-BURN was also used to generate the photosynthetic vegetation fraction (PV), for analysis of fire effects on canopy cover (Asner et al. 2005b). These images were also used to map annual changes in forest cover due to deforestation (Alencar et al. 2011).

To calculate the fire seasonality, we used a monthly hot pixel database derived from the NOAA 11, 12, and 15 satellites. This database includes 16 years (1992-2007) of monthly dry season fire counts (June to November) for the three study regions. These data are part of the national fire database available on the Brazilian National Space Agency (INPE) webpage (http://www.dpi.inpe.br/proarco/bdqueimadas/). Together, the two types of remote sensing derived datasets were used to calculate fire extent, frequency, return interval, and effects on canopy cover, as well as to evaluate changes in fire seasonality.

Fire Sizes and Overall Extent

The forest area burned from 1983 to 2007 was calculated using annual burn scar maps derived from CLAS-BURN for the three forest regions. To do so, we first excluded from our analysis savanna and other types of non-forest vegetation. Next, the number and the sizes of individual fire scar polygons per year, were used to generate annual burn data. Descriptive statistics and analysis of variance were calculated for the individual fire scars to assess the main differences between the three forest types and the temporal changes within each region.

Fire Frequencies and Fire Return Interval

For each of the three study regions, all annual burn scar maps were stacked into a single frequency map, providing a probability distribution of burn scar size classes. The mean number of repeated fires (MRF) for dense, open, and transitional forest were also calculated from the relationship between the total area burned at least once during the 24 yrs of annual observations, without recounting multiple burns of the same site, and the sum of the annual total area burned during that same period, including all reburns. The fire return interval was also retrieved for each burned pixel in the time-series for each region to create a distribution of the area burned assembled by the time since last fire. We used the fire interval data to calculate the maximum number of years in which a given area burned (Maximum Fire Recurrence – MFR). Fire rotation time (FR) was also calculated, which expresses the time necessary for the study areas to burn entirely based on the average annual burned area, assuming that some areas will not burn while others may burn multiple times (Cochrane et al. 1999).

Fire Seasonality

We assessed fire seasonality for the three study regions with a monthly hot pixel time series derived from NOAA 11, 12, and 15. Due to lack of high resolution multispectral images without clouds needed to map monthly forest burn scars, we used hot pixels as a proxy for forest fire seasonality; this use of hot pixels seems justified insofar as they represent the actual time when fire ignition from burned pastures and swidden agriculture occur, which are the main sources of Amazon forest fires (Schroeder et al. 2005). Two measurements of seasonality were extracted from this dataset, one that describes the average peak of fire activity over the 16-year period of monitoring (1992-2007) and the other that reveals time shifts in that peak.

Repeated Fire Effects on Canopy Cover

We evaluated fire effects as a proxy for accumulated fire severity by taking into account the impacts of different number of repeated burns on forest canopy cover, as retrieved from satellite-based estimates. The “fraction of forest canopy cover” metric of Asner *et al.* (2004, 2005b) derived from the fraction of Photosynthetic Vegetation (PV) existing in a pixel, was used to quantify the impacts on canopy openness after different intensities of selective logging. These satellite estimates of forest canopy cover have a strong inverse relationship with canopy gap fraction measured in the field (Asner et al. 2004). The satellite-derived measurements were generated from a sub-pixel fraction algorithm called

Carnegie Landsat Analysis System (CLAS) that decomposes a pixel into fractions of photosynthetic vegetation or forest canopy cover (PV), non-photosynthetic vegetation (NPV), and soil (Asner et al. 2004). The Asner et al. (2005) approach was used to derive satellite-based forest canopy cover from the PV fraction retrieved from CLAS-BURN spectral mixing analysis, where the soil fraction was replaced by the shade-burn fraction (Alencar et al. 2011). Shade-burn fraction increases in forest canopy pixels recently affected by understory fires due to the heterogeneity of materials found in a recently burned forest (i.e. ashes, charcoal, increase dead wood material).

The impacts of different fire frequencies on forest canopy cover were measured for the three forest types. Measurements of satellite-based forest canopy cover (PV) were extracted for seven levels of fire repetition (burned from 0 to 6 times) using a random sampling routine and the 2008 images for all study regions (350 samples for each fire frequency). The samples located in areas burned in 2007 were excluded to avoid the strong signal of recent burned materials such as charcoal and ash (Alencar et al. 2011). These measurements generated a probability distribution of fire effects that varied with number of reburns for each forest type.

Climate Data and Fire Regime Metrics

To evaluate some of the effects of weather variability on fire regimes, we used the Standardized Precipitation Index (SPI) and El Niño Southern Oscillation ENSO indexes. SPI, which is based on monthly precipitation data, indicates dry and wet conditions (McKee et al. 1993). This index represents a standardized probability density function of precipitation following a normal distribution. Zero standard deviation indicates median precipitation condition, while extreme negative and positive standard deviations indicate drought and wet conditions respectively. SPI data from the analysis period were compiled from Adler et al. (2003). We also used a consensus combination of Oceanic Nino Index (ONI), Multivariate ENSO Index (MEI) to categorize the years of Strong, Moderate and Weak El Nino and La

Nina (http://ggweather.com/enso/years.htm). We related these climatic variables to the annual fire metrics area burned, burn scar size, and number of fire scars.

Results

Fire Extent

From 1983-2007, fires burned large portions of eastern Amazonian forests, but the extent varied with forest type and year. Dense forest was the least affected by fire, burning three-times less than open and transitional forests. Forest fires burned 0.33 billion ha of dense forest compared to 1 billion ha of open, and 0.56 billion ha of transitional forests that represent, respectively, 15%, 44%, and 46% of the standing forests of each type in these study regions (Table 2).

During the 24 yr observation period, 29% of dense, 54% of open, and 50% of transitional forests were lost to deforestation (Table 1); 19%, 39%, and 38% of the deforested area in these three forest types, respectively, were burned one or more years prior to clearing (Table 2). However, the proportions of the burned areas that were subsequently deforested in these three study regions (6% dense, 21% open, and 19% transitional) did not explain deforestation in all the years studied (Fisher's exact tests, P = 0.63, 0.45 and 0.7).

The area affected by forest fires varied substantially among years. The annual distribution of area burned indicates a tendency towards increased forest area affected by fire over the last 10 years of observation (1997-2007) in all the regions (Figure 2), but this trend was significant only for open forest (P = 0.03). Although less dense forest burned than open or transitional forest, it was the forest type with greatest inter-annual variation in area burned. While there were 70- and 100-fold differences between the minimum and maximum area burned annually for transitional and open forest, respectively, the ratio was 1200 for dense forest (Table 3). The mean annual burned areas (MBA) were 19,900 ha, 104,700 ha, and

80,000 ha for dense, open, and transitional forests, respectively (Table 3). For the dense forest, the average annual burned area was 35% less than the annual deforestation rate, whereas the average forest area burned in open and transitional forests were, respectively, 70% and 180% greater than the annual area deforested (Tables 2 and 3).

Fire Size and Number

The size and number of individual fires varied substantially among years in the three forest types. In general, the number of fire scars, as well as the size of individual fire scars, varied more in the dense forest than in the other forest types (Table 3). While the mean number of fire scars (MNFS) was in absolute numbers similar in dense and transitional forest (774 and 720 individual fire scars on average), when normalized by the total forest area, the number of individual fire scars was about the same in transitional and open forests and these two forest types had ~60% more than the annual number of fire scars found in dense forest. The mean maximum fire size (MMFS) - the average size of the largest fire scar in each year - was 1,311 ha in dense forest, which is about 10 times smaller than the maximum fire sizes in the other forest types (Table 3).

Despite between year variability, about 80-90% of the annual fire scars were <100 ha. Although the majority of fire scars were small in all three regions, fire scar size classes occupied different proportions of the burned landscape in each region (Figure 3). Large fires (> 1000 ha) accounted for a larger percentage of total burned area in transitional and open forests than in dense forests (Figure 3). In contrast, small fires (< 100 ha) accounted for larger proportion of dense forests burn area than in other forest types. Medium size fires (100 – 1000 ha) also affected a large area of dense forest but, burned approximately the same proportions of transitional and open forest (Figure 3).

Fire Frequency and Burn Intervals

Most of the burned forests did not experience repeated fires at the same site during the 24-year observation period. When the total burned area was classified by number of repeated fires, the proportion of this total burned area decreased as fire frequency increased. Although this pattern was consistent among the three forest types, reburning was less common in dense forest (Figure 4). For example, the proportion of total burned area that was burned only once was 72% in dense forest, but only 45% and 30% in open and transitional forests, respectively. Two burns within the 24-year period comprised the second most common class and occupied similar proportions of the total burned area of all forest types (20%, 24%, and 22% in dense, open, and transitional forests, respectively). Most areas that experienced many repeated fires are along major roads or near human settlements and fire-prone vegetation types (e.g., savanna; Figure 1). These results indicate that dense forest was least likely to burn repeatedly, whereas transitional forest burned with much higher frequencies, up to 12 times over the 24-year observation period (0.5% of the total area burned). The maximum number of consecutive years during which a given area burned was three for dense, nine for open, and six for transitional forest (Table 3). Although these annual recurrences are high for open and transitional forests, they represented less than 0.5% of the total area burned. These frequency distributions expressed as mean number of repeated fires (MRF) was found to be 1.4 times for dense, 2.3 times for open, and 3.1 times for transitional forests during the period of analysis (Table 3), with fire rotation times of 82 yr, 15 yr, and 11 yr for dense, open and transitional forests, respectively, in a scenario of no deforestation (Table 3).

Fire Seasonality

The sum of the total fire season hot pixel counts for each year was positively correlated with the total annual area deforested ($R^2 = 0.25$; $P < 0.0001$). That correlation strengthened when the annual burned forest area was added ($R^2 = 0.35$; $P < 0.0001$). This suggests that hot pixels detect fire not only in open deforested areas, but also in standing forests. In addition, monthly hot pixel counts decreased with increasing monthly rainfall in the three forest types, but only significantly so in the dense forest region ($R^2 = 0.29$; $P = 0.04$). Hot pixel counts were much higher in the open forest region than in the area of dense or transitional forests (Figure 5). In addition, fire seasonality, as measured by these ignition source peaks, differed among the three forest types. This peak usually precedes the rainy season and therefore tends to be influenced by dry season duration. Based on the fire peak assumption, dense forest had October and November as the months with highest hot pixel counts from 1992 to 2007 compared to August and September peaks in the more southern locations of open and transitional forests, preceding the rainy season starting in December in the dense forest region and October in the other forest regions (Villar et al. 2009).

Historical analysis of changes in the percentage of total annual hot pixel counts for the two months with highest fire activity demonstrated slight shifts in the fire season from one month to the other for the three forest types (Figure 5). In dense forest, hot pixel counts decreased with time ($P < 0.01$) and were lower in October than November. In comparison, fire activity in the open forest region significantly decreased in August ($P = 0.02$) and then increased substantially in September ($P = 0.01$), suggesting that the fire season peak shifted to later in the dry season. The transitional forest also witnessed a strong decrease in August ($P = 0.03$) fire counts over time, but much less of an increase in September ($P = 0.60$). All these results suggest that the peak of fire activity is shifting towards later months when is drier, which may have major impact on fire extent, size, and effects.

Fire Effects on Canopy Cover

Forests that burned more often tended to have more open canopies as indicated by a negative relationship between forest canopy cover (PV) and mean number of repeated fires

(MRF; Figure 6). Although PV generally decreased with increased fire frequency, the relationships were remarkably different among the forest types.

Forest canopy cover in the dense forest decreased markedly at the highest frequencies reported (burned 4, 5, and > 6 times) (Figure 6). Despite the strong statistical relationship between canopy cover and fire frequency in this forest type ($P < 0.0001$), satellite-based measurements of forest canopy cover failed to differentiate impacts of old lower burn frequencies (1-3 times burned) from the unburned forest canopy cover (Figure 6).

Fire frequency in open forest was weaker than in dense forest, but still inversely significant related to canopy cover ($P < 0.0001$). In this forest type, the distribution of canopy cover by number of repeated fires significantly declined only after the fourth burn, with the effect on canopy cover being very evident for forests burned more than six times. Transitional forest showed the largest effect of fire frequency on forest canopy cover. Although the difference in forest canopy cover between unburned and once burned areas was small for this forest type, higher fire frequencies opened the canopy substantially (Figure 6).

Forest Fire Regime, Climate and Deforestation

Total area burned, number of fire scars, and maximum size of fire scars were positively inter-correlated and all inversely correlated with fire rotation time for the three forest types (Spearman's $p < 0.05$; Table 4). In dense forests, most fire regime metrics were strongly responsive to ENSOs, when more area burned, forming more and larger fire scars and more fire scars (Figure 7 a). For open and transitional forests, in contrast, linkages between fire regime properties and extreme weather events were less apparent. For these two forest types, more area burned (relative to the total standing forest), burn scars were larger, and a greater number of individual fires scars were observed during non-ENSO or moderate ENSO years (Figure 7 b, c), These patterns indicate that forest fires in open and transitional forests were also strongly influenced by deforestation rates, which were much higher than in dense forests. When we conducted our analysis using SPI data, (Figure 7 d, e, f), the results were similar.

Discussion

Spatial-temporal analysis of forest fire regime metrics indicates that interactions between extreme weather events and agricultural practices drove the recently observed variability in Amazon forest fire regimes along the Eastern border of the region. Between 1983 and 2007, drought events triggered forest fires that were larger, more frequent, and that spanned over a wider range of dry-season months, probably causing increased fire-induced tree mortality as well (Brando et al. 2014). These changes in fire-regime properties were more pronounced in forest areas where land use change caused forest fragmentation, and where sources of fire ignition were abundant along the 'arc of deforestation' in open canopy and transitional forests. One of our most striking results was the temporal change in fire regimes across different forest types of the Amazon. While the Amazon fire regime intensified overall, this trend was mostly associated with the vulnerability of transitional and open forests to fire, even during wetter-than-average years. In contrast, dense forests burned mostly during extreme dry years (e.g., ENSOs in the 80s and 90s and an AMO in the 2000s; (Marengo et al. 2013). These differences in fire regime properties between open/transitional and dense forests indicate that human activities have greater influence on the fire regimes of transitional and open forest sites, which are being converted rapidly into agricultural fields and pasture (Figure 7).

Contrary to the widely accepted notion that the fuel bed of Amazonian forests is too humid to catch fire in non-drought years, large areas of transitional and open Amazonian forests burned during the 2000s under average-weather conditions, and at a rate that was higher than in the earlier decades of analysis (Alencar et al. 2006). This pattern in eastern Amazon forest fires likely results from a combination of factors: (i) increasing dry-season temperature and decreasing rainfall (Malhi et al. 2008); (ii) cumulative annual rainfall reduction (Nepstad et al. 2004) promoted by climatic cycles besides ENSO such as AMO (Chen et al. 2011); and (iii) increased forest fragmentation due to high rates of deforestation (Broadbent et al. 2008) - deforestation rates were much higher in open forest than in transitional and dense forests. The observed increases in burned area over time, even as deforestation rates decreased, suggest that weather probably overwhelmed the expected inhibitory effect of reduced fire ignition sources that often accompany deforestation.

Increasing Anthropogenic Amazon Fire Regimes

Our results show that spatial and temporal variability in fire-regime properties are interconnected, with the temporal fire regime domains (e.g., frequency, interval, and seasonality) influencing the spatial ones (e.g., area burned, size and number of individual burn scars) (Falk et al. 2007). As precipitation decreases, for example, dry season length typically increases (Fu et al. 2013), and the timing of anthropogenic ignitions for deforestation and pasture and crop management shift to later in the season. Fires ignited late in the dry season of a dry year are more likely to spread further into intact forest, which is itself more susceptible to fire at such times (Nepstad et al. 2004).

Across our study sites, ignition fires are occurring later in the dry season and with greater variability in extremely dry years, most significantly in the open forest region. These tendencies and shifts increase the potential for extensive forest fires, both in terms of total area burned and the size of individual burns. Open forests, followed by transitional forests, were most affected by changes in fire seasonality, and also faced more area burned with fire scars ten times larger on average than in dense forest. Morton et al.(2011) also reported larger fires in southern Amazonia, dominated by transitional and open forest types, than in the northeastern part of the region dominated by dense forest, but using a shorter time-series. These differences between forest types may result from increases in ignition sources in open and transitional forests related to large-scale deforestation, as well as from the enhanced natural vulnerability to fire of these forests as compared to dense forest, which is more humid and climatologically less seasonal.

The extent, size, and number of fires are all correlated with one another, and with fire intensity and frequency, because they all affect and are affected by fuel conditions. As a result, landscapes with fewer fires but large fire scars are expected to burn more intensely. This study also confirms the reported relationship between fire frequency and fire effects as measured by changes in canopy cover (Cochrane and Schulze 1999, Barlow and Peres 2008), but we also found that the effects of repeated fires in transitional forest are particularly severe if compared to open and dense forests, which tend to respond to dramatic changes in canopy cover mostly at higher fire frequencies.

The high fire recurrence rates observed in transitional and open forests are most likely related to their proximity to ignition sources and are compatible with the patterns described for the southern Amazon by Morton et al. (2013). While subsequent fires in open forest are spatially associated with roads and settlements (78% of the consecutive fires happened within 10 km of a settlement), recurrent fires in transitional forests mostly occurred on the borders of savannas that naturally experience high fire frequencies. The relationship between high fire recurrence rates and proximity to roads, edges of forest clearings, and settlements is supported by the Fire Rotation time (FR) results, which increased from 7 yrs (reported in Cochrane et al. (1999) for a smaller portion of the dense forest study site located along a main road and within a settlement occupation) to 82 yrs for the entire dense forest site, which also include remote areas. This indicates the sensitivity of this metric to the size and location of the area studied and supports the hypothesis that high fire recurrence rates occur mostly on edges of deforested areas.

The coupled effects of a drier future climate, with more ignition sources in increasingly fragmented landscapes, can decrease the fire resistance of even dense evergreen forest. Our results indicate that these changes are already underway, with changes in major spatial and temporal domains of Amazonian fire regimes, even as strict government control has recently reduced deforestation (Nepstad et al. 2014). If proactive fire policies are not enacted to promote sustainable land uses that keep the rates of deforestation low and reduce forest degradation and ignition sources (e.g. pasture and agriculture management fires), emissions from forest fires will likely double or even triple due to more frequent and intense burns.

Conclusions

We developed a 24-yr time series of forest fire scar maps from satellite-based measurements to reveal changing fire regime properties in three distinct forest types in the eastern Amazon basin. Our study revealed that forest fires have already increased in response to drought and increasing deforestation, forest fragmentation, and forest degradation. Forest fires were also found to affect different proportions of each common forest type found throughout the region, with transitional and open forests being most prone to larger and more frequent burns even in relatively wet years.

The effects of climate change and other human-driven factors on forest fire susceptibility varied among forest types. On one hand, dense forest is very sensitive to changes in climate, although landscape changes such as fragmentation exacerbate this susceptibility. In contrast, the fire regimes of transitional and open forests, although sensitive to changes in climate and particularly drought, are more sensitive to increases in ignition sources and changes in forest cover due to forest fragmentation. These naturally drier forests demonstrated to be less resistant but perhaps more resilient to fire, as demonstrated by larger areas burned, at higher frequencies, and at shorter fire intervals.

Increasing forest fires cause large-scale forest degradation and enhances carbon emissions to rates three or four times the annual deforestation emissions from some forest types (Alencar et al. 2006). Our results inform predictions of the future of tropical forest landscapes subjected to climate change and anthropogenic fires. Policies that address fire reduction through both deforestation reduction and modified land management practices are now needed in response to irreversible climate warming.

Acknowledgements

This work was supported by NSF-DDRIG award 0727220, NASA NESSF Program Grant NNX07AN76H, NSF DEB-0410315, NSF DEB-1146206, the Compton Foundation, the Gordon and Betty Moore Foundation, the John D. and Catherine T. MacArthur Foundation, and the Tropical Conservation and Development Program and the Amazon Conservation Leadership Initiative Program at the University of Florida. We thank Douglas Morton, Daniel Zarin and Wendell Cropper for comments on early versions of this study.

Literature Cited

Adler, R. F., G. J. Huffman, A. Chang, R. Ferraro, P. Xie, J. Janowiak, B. Rudolf, U. Schneider, S. Curtis, D. Bolvin, A. Gruber, J. Susskind, and P. Arkin. 2003. The Version 2 Global Precipitation Climatology Project (GPCP) Monthly Precipitation Analysis (1979-Present). Journal of Hydrometeorology **4**:1147-1167.

Alencar, A., G. P. Asner, D. E. Knapp, and D. J. Zarin. 2011. Temporal variability of forest fires in eastern Amazon. Ecological Application **21**:2397-2412.

Alencar, A., D. Nepstad, and M. C. Vera Diaz. 2006. Forest understory fire in the Brazilian Amazon in ENSO and non-ENSO Years: area burned and committed carbon emissions. Earth Interactions **10**:1-17.

Alencar, A., L. Solorzano, and D. Nepstad. 2004. Modeling Forest Understory Fires in an Eastern Amazonian Landscape. Ecological Applications **14**:S139-S149.

Aragão, L., Y. Malhi, R. M. M. Roman-Cuesta, S. Saatchi, L. O. O. Anderson, and Y. E. E. Shimabukuro. 2007. Spatial patterns and fire response of recent Amazonian droughts. Geophys. Res. Lett. **34**: 1-5.

Aragão, L. E. O. C., Y. Malhi, N. Barbier, A. Lima, Y. E. Shimabukuro, L. O. Anderson, and S. Saatchi. 2008. Interactions between rainfall, deforestation and fires during recent years in the Brazilian Amazonia. Phil. Trans. R. Soc. **363**:1779-1785.

Aragão, L. E. O. C., and Y. E. Shimabukuro. 2010. The incidence of fire in Amazonian Forests with implications for REDD. Science **328**:1275-1278.

Asner, G. P., M. Keller, R. Pereira, J. C. Zweede, and J. N. M. Silva. 2004. Canopy damage and recovery following selective logging in an Amazon forest: Integrating field and satellite studies. Ecological Applications **14**:280-298.

Asner, G. P., D. E. Knapp, E. N. Broadbent, P. J. C. Oliveira, M. Keller, and J. N. Silva. 2005a. Selective Logging in the Brazilian Amazon. Science **310**:480 - 482.

Asner, G. P., D. E. Knapp, A. N. Cooper, M. C. C. Bustamante, and L. O. Olander. 2005b. Ecosystem structure throughout the Brazilian Amazon from Landsat data and spectral unmixing. Earth Interactions **9**:1-31.

Baccini, A., S. W. Goetz, W. S. Walker, N. T. Laporte, M. Sun, D. Sulla-Menashe, J. Hackler, P. S. A. Beck, R. Dubayah, M. A. Friedl, S. Samanta, and R. A. Houghton. 2012. Estimated carbon dioxide emissions from tropical deforestation improved by carbon-density maps. Nature Climate Change **2**: 1-4.

Barlow, J., and C. A. Peres. 2008. Fire-mediated dieback and compositional cascade in an Amazonian forest. Phil. Trans. R. Soc. **363**:1787-1794.

Bowman, M. S., B. S. Soares Filho, F. D. Merry, D. C. Nepstad, H. Rodrigues, and O. T. Almeida. 2012. Persistence of cattle ranching in the Brazilian Amazon: A spatial analysis of the rationale for beef production. Land Use Policy **29**:558-568.

Broadbent, E. N., G. P. Asner, M. Keller, D. E. Knapp, P. J. C. Oliveira, and J. N. Silva. 2008. Forest fragmentation and edge effects from deforestation and selective logging in the Brazilian Amazon. Biological Conservation **141**:1745-1757.

Bush, M. B., M. R. Silman, C. McMichael, and S. Saatchi. 2008. Fire, climate change and biodiversity in Amazonia: a late-Holocene perspective. Phil. Trans. R. Soc. **363**:1795-1802.

Chen, Y., J. T. Randerson, D. C. Morton, R. S. DeFries, J. G. Collatz, P. S. Kasibhatla, L. Giglio, Y. Jin, and M. E. Marlier. 2011. Forecasting Fire Season Severity in South America Using Sea Surface Temperature Anomalies. Science **334**:787-791.

Cochrane, M., A. Alencar, M. Schulze, C. Souza Jr, D. C. Nepstad, P. Lefebvre, and E. Davidson. 1999. Positive Feedbacks in the Fire Dynamic of Closed Canopy Tropical Forest. Science **284**:1837-1841.

Cochrane, M., and W. F. Laurance. 2002. Fire as a large-scale edge effect in Amazonia forests. Journal of Tropical Ecology **18**:311-325.

Cochrane, M. A., and W. F. Laurance. 2008. Synergisms among fire, land use, and climate change in the Amazon. Ambio **37**:522-527.

Cochrane, M. A., and M. D. Schulze. 1999. Fire as a recurrent event in tropical forests of the eastern Amazon: effects on forest structure, biomass, and species composition. Biotropica **31**:2-16.

Da Silva, R. R., D. Werth, and R. Avissar. 2008. Regional impacts of future land-cover changes on the Amazon basin wet-season climate. Journal of Climate **21**:1153-1170.

Davidson, E. a., A. C. de Araújo, P. Artaxo, J. K. Balch, I. F. Brown, M. M. Bustamante, M. T. Coe, R. DeFries, M. Keller, M. Longo, J. W. Munger, W. Schroeder, B. Soares Filho, C. Souza Jr, and S. C. Wofsy. 2012. The Amazon basin in transition. Nature **481**:321-328.

Falk, D. A., C. Miller, D. McKenzie, and A. E. Black. 2007. Cross-Scale Analysis of Fire Regimes. Ecosystems **10**:809-823.

Fearnside, P. M. 2005. Deforestation in Brazilian Amazonia : History , Rates , and Consequences. Conservation Biology **19**:680–688.

Fu, R., L. Yin, W. Li, P. A. Arias, R. E. Dickinson, L. Huang, S. Chakraborty, K. Fernandes, B. Liebmann, R. Fisher, and R. B. Myneni. 2013. Increased dry-season length over southern Amazonia in recent decades and its implication for future climate projection. PNAS **110**:18110-18115.

Lentini, M., D. Pereira, D. Celentano, and R. Pereira. 2005. Fatos Florestais da Amazonia 2005. IMAZON, Belém.

Lewis, S. L., P. M. Brando, O. L. Phillips, G. M. F. van der Heijden, and D. Nepstad. 2011. The 2010 Amazon drought. Science **331**:554.

Macedo, M. N., R. S. DeFries, D. C. Morton, C. M. Stickler, G. L. Galford, and Y. E. Shimabukuro. 2012. Decoupling of deforestation and soy production in the southern

Amazon during the late 2000s. Proceedings of the National Academy of Sciences **109**:1341-1346.

Malhi, Y., T. Roberts, R. A. Betts, T. J. Killeen, W. Li, and C. A. Nobre. 2008. Climate Change, Deforestation, and the Fate of the Amazon. Science **319**:169-172.

Marengo, J. A., L. M. Alves, W. R. Soares, D. A. Rodriguez, H. Camargo, M. P. Riveros, and A. D. Pabló. 2013. Two Contrasting Severe Seasonal Extremes in Tropical South America in 2012: Flood in Amazonia and Drought in Northeast Brazil. Journal of Climate **26**:9137-9154.

Marengo, J. A., J. Tomasella, L. M. Alves, W. R. Soares, and D. A. Rodriguez. 2011. The drought of 2010 in the context of historical droughts in the Amazon region. Geophys. Res. Lett. **38**: 3-5.

McKee, T. B., N. J. Doeskin, and J. Kleist. 1993. The relationship of drought frequency and duration to timescales. Pages 179-184 *in* 8th Conf. on applied climatology. American Meteorological Society, Anaheim, Canada.

Meggers, B. J. 1994. Archeological evidence for the impact of Mega-Niño events of Amazonia during the past two millennia. Climatic Change **28**:321-338.

Merry, F., B. Soares-Filho, D. Nepstad, G. Amacher, and H. Rodrigues. 2009. Balancing conservation and economic sustainability: the future of the Amazon timber industry. Environmental Management **44**:395–407.

Morton, D. C., R. S. DeFries, J. Nagol, C. M. Souza, E. S. Kasischke, G. C. Hurtt, and R. Dubayah. 2011. Mapping canopy damage from understory fires in Amazon forests using annual time series of Landsat and MODIS data. Remote Sensing of Environment **115**:1706-1720.

Morton, D. C., Y. Le Page, R. DeFries, J. G. Collatz, and G. C. Hurtt. 2013. Understorey fire frequency and the fate of burned forest in southern Amazonia. Phil. Trans. R. Soc. B **368**:20120163.

Nepstad, D., P. Lefebvre, U. Lopes da Silva, J. Tomasella, P. Schlesinger, L. Solórzano, P. Moutinho, D. Ray, and J. Guerreira Benito. 2004. Amazon drought and its implications for forest flammability and tree growth: a basin-wide analysis. Global Change Biology **10**:704-717.

Nepstad, D., D. McGrath, C. Stickler, A. Alencar, A. Azevedo, B. Swette, T. Bezerra, M. DiGiano, J. Shimada, R. Seroa da Mota, E. Armijo, L. Castello, P. Brando, M. C. Hansen, M. Mcgrath-Horn, O. Carvalho, and L. Hess. 2014. Slowing Amazon deforestation through public policy and interventions in beef and soy supply chains. Science **344**: 1118–1123.

Pacheco, P. 2009. Agrarian Reform in the Brazilian Amazon: Its Implications for Land Distribution and Deforestation. World Development **37**:1337–1347.

RADAMBRASIL. 1981. Levantamento de Recursos Naturais 1973-1984.*in* D. N. d. P. Mineral, editor. IBGE, Rio de Janeiro.

Sanford, R. L., J. Saldarriaga, K. Clark, C. Uhl, and R. Herrera. 1985. Amazon rain-forest fires. Science **227**:53-55.

Schroeder, W., J. T. Morisette, I. Csiszar, L. Giglio, D. Morton, and C. O. Justice. 2005. Characterizing Vegetation Fire Dynamics in Brazil through Multisatellite Data: Common Trends and Practical Issues. Earth Interactions **9**:1-26.

Souza, J., C., J. Siqueira, M. Sales, A. Fonseca, J. Ribeiro, I. Numata, M. A. Cochrane, C. P. Barber, and J. Barlow. 2013. Ten-Year Landsat Classification of Deforestation and Forest Degradation in the Brazilian Amazon. Remote Sensing **5**:5493–5513.

Thonicke, K., S. Venevsky, S. Sitch, and W. Cramer. 2001. The role of fire disturbance for global vegetation dynamics: coupling fire into a Dynamic Global Vegetation Model. Global Ecology & Biogeography **10**:661-677.

Villar, J. C. E., J. Ronchail, J. L. Guyot, G. Cochonneau, F. Naziano, W. Lavado, E. De Oliveira, R. Pombosag, and P. Vauchelh. 2009. Spatio-temporal rainfall variability in the Amazon basin countries (Brazil, Peru, Bolivia, Colombia, and Ecuador). International Journal of Climatology **29**:1574-1594.

Yoon, J. H., and N. Zeng. 2010. An Atlantic influence on Amazon rainfall. Climate Dynamics **34**:249–264.

Zeng, N., J. Yoon, J. Marengo, A. Subramaniam, C. A. Nobre, A. Mariotti, and J. D. Neelin. 2008. Causes and impacts of the 2005 Amazon drought. Environmental Research Letters **3**:1-9.

Table 1. Principal characteristics of each of three forest types encountered in the eastern Amazon basin.

Forest Type	Average Biomass (ton ha^{-1})	Average annual Rainfall (mm)	Dominant Land Use	% of Landscape Deforested
Dense	350	2,200	cattle ranching, agricultural settlements and selective logging	29
Open	250	1,700	large scale cattle ranching and recent history of settlement occupation	54
Transitional	200	1,300	large scale cattle ranching, mechanized agriculture and recent history of settlement occupation	50

Table 2. Annual burned and deforested areas from 1983 to 2007 for three Eastern Amazon study regions dominated by dense, open, and transitional forests (* Total forest area mapped at the beginning of the time series in 1984 for open and transitional forest, and 1983 for dense forest).

	Forest area (ha)*	Total Burned Area (ha)	Total area deforested between 1983-2007 (ha)	Average annual deforestation (ha)	% of total forest area burned	% of forest loss between 1983 -2007	% of total area deforested that burned
Dense	2,274,133	333,345	834,235	29,393	15%	37%	19%
Open	2,324,883	1,027,649	1,286,294	62,821	44%	55%	39%
Transitional	1,241,640	565,095	588,473	27,901	46%	47%	38%

Table 3. Summary of spatial and temporal fire regime properties by forest type. Numbers in parentheses represent the standard deviations of the average value.

	Fire regime properties	Dense forest	Open forest	Transitional forest
Spatial fire regime characteristic	Mean annual burned area - MBA (ha)	19,932 (5,931)	104,711 (20,444)	80,189 (17,013)
	Min and Max annual burned area (ha)	92 - 117,656	3,171 - 326,964	4,421 - 312,777
	Mean annual number of fire scars - MNFS	774 (225)	1,247 (133)	720 (126)
	Mean annual maximum fire size - MMFS (ha)	1,311 (397)	12,850 (3,367)	13,804 (3,145)
Temporal fire regime characteristic	Mean number of repeated burns - MRF (number of fires in 23 years)	1.4 (0.72)	2.3 (1.8)	3.1 (2.1)
	Maximum annually consecutive fire recurrences -MFR (years)	3	9	6
	Fire Rotation -FR (years)	82	15	11

Table 4. Spearman's correlation between spatial fire regime properties and climate variables (ENSO Class as determined by ONI and MEI indexes, and Standardized Precipitation Index - SPI). Significant correlations are indicated in the table (* Spearman's P < 0.05).

	Area burned	Number of fire scars	Max. scar size	%forest burn	Fire rotation	ENSO Class	SPI
Area burned	1.00						
Number of fire scars	0.95*	1.00					
Max. scar size	0.94*	0.91*	1.00				
% forest burn	0.92*	0.86*	0.87*	1.00			
Fire rotation	-0.99*	-0.95*	-0.94*	-0.92*	1.00		
ENSO Class	0.43*	0.48*	0.47*	0.33	-0.45*	1.00	
SPI	-0.41	-0.40	-0.37	-0.31	0.42*	-0.80*	1.00
Area burned	1.00						
Number of fire scars	0.86*	1.00					
Max. scar size	0.91*	0.83*	1.00				
% forest burn	0.97*	0.88*	0.91*	1.00			
Fire rotation	-0.98*	-0.88*	-0.90*	-1.00*	1.00		
ENSO Class	0.15	0.28	0.12	0.10	-0.10	1.00	
SPI	-0.21	-0.38	-0.17	-0.21	0.21	-0.77*	1.00
Area burned	1.00						
Number of fire scars	0.72*	1.00					
Max. scar size	0.91*	0.57*	1.00				
% forest burn	0.97*	0.76*	0.89*	1.00			
Fire rotation	-0.97*	-0.75*	-0.90*	-0.99*	1.00		
ENSO Class	0.42	0.36	0.35	0.35	-0.33	1.00	
SPI	-0.06	0.12	-0.17	-0.02	0.02	-0.30	1.00

Figure Legends

Figure 1. Study site locations by forest type (a) Dense forest, (b) Open forest and (c) Transitional forest, showing the spatial distribution of the forest areas affected by fire and color coded by number of repeated fires from 1983 to 2007.

Figure 2. Proportions of remaining forest areas burned by year in the Dense, Open and Transitional forests. The thin line is the mean trend of burned areas over the years for dense forest, the dotted line for open forest ($R^2 = 0.206$; $P = 0.03$), and the thick line for transitional forest.

Figure 3. Proportion of total area burned by fire scar size and forest type.

Figure 4. Proportion of the burned area affected by different burn frequencies by forest type.

Figure 5. Trend of satellite hot-pixels for the two months of highest fire incidence and prior to the raining season in (a) dense (October and November; $P < 0.001$ and $P = 0.92$), (b) open (August and September; $P = 0.02$ and $P = 0.01$) and (c) transitional forest regions (August and September; $P = 0.03$ and $P = 0.60$).

Figure 6. Relationship between canopy cover as measured by sub-pixel fraction photosynthetic vegetation material (PV) representing forest canopy cover and number of repeated fires for Dense, Open and Transitional forests.

Figure 7. Relationship between the proportion of burned area, maximum size of burned area and number of burn scars (circle size). The color scales represent the intensity of ENSO (Dark and pale red – Strong and Moderate ENSO; Gray –Weak ENSO; Blue – No ENSO) and of SPI values ranging from -3 (dark red) to 1.6 (blue), for (a) and (d) dense forest, (b) and (e) open forest, and (c) and (d) transitional forest.

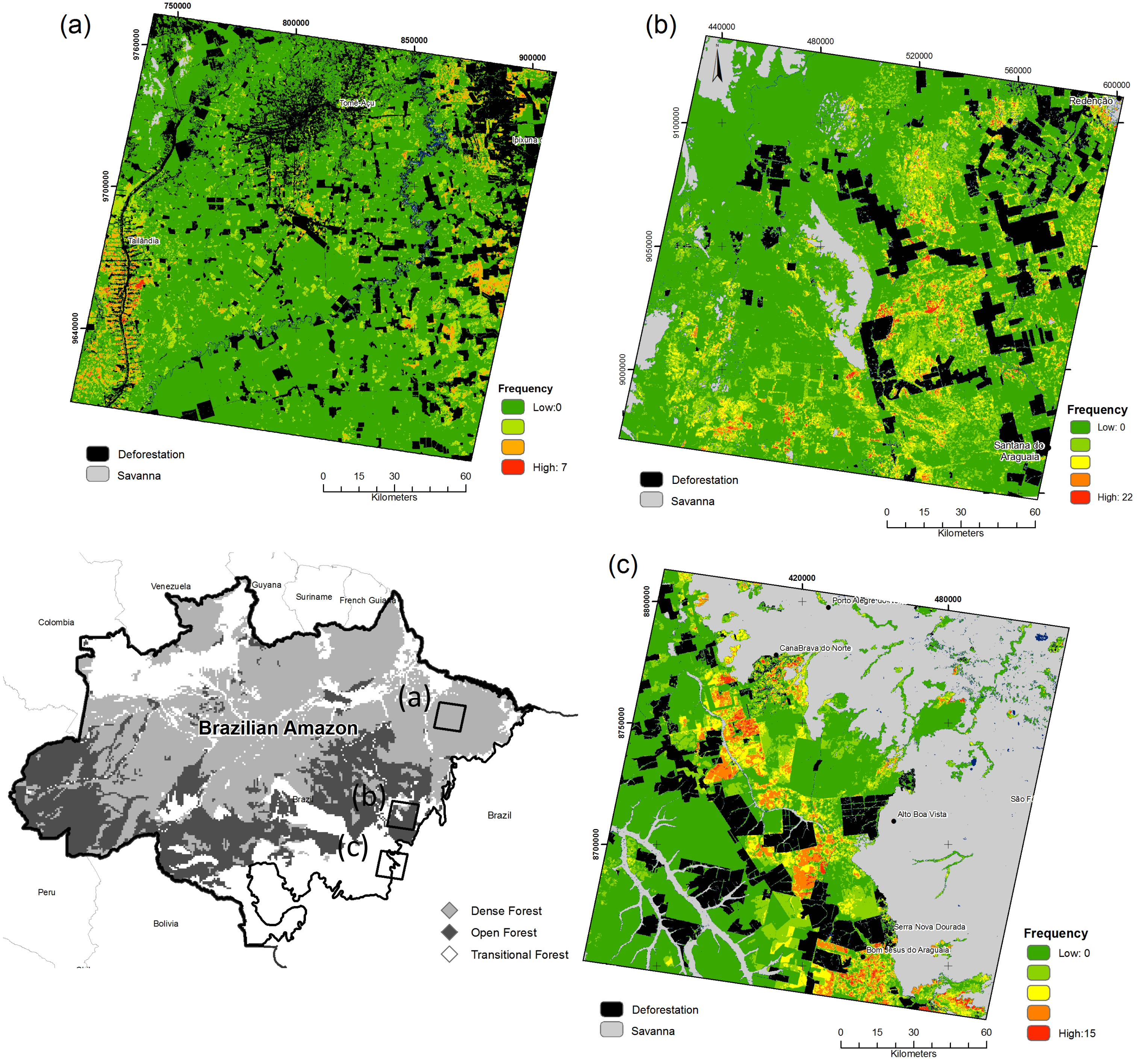
(a)
750000
800000
850000
900000
9760000
9700000
9640000
Tomé-Açu
Ipixuna
Tailândia
Frequency
🟩 Low:0
🟥 High: 7
⬛ Deforestation
⬜ Savanna
0
15
30
60
Kilometers
(b)
440000
480000
520000
560000
600000
9100000
9050000
9000000
Redenção
Santana do Araguaia
Frequency
🟩 Low: 0
🟥 High: 22
⬛ Deforestation
⬜ Savanna
0
15
30
60
Kilometers
Venezuela
Guyana
Suriname
French Guiana
Colombia
Brazilian Amazon
(a)
(b)
(c)
Brazil
Brazil
Peru
Bolivia
◆ Dense Forest
◆ Open Forest
◇ Transitional Forest
(c)
420000
480000
8800000
8750000
8700000
Porto Alegre
CanaBrava do Norte
Alto Boa Vista
Serra Nova Dourada
Bom Jesus do Araguaia
Frequency
🟩 Low: 0
🟥 High:15
⬛ Deforestation
⬜ Savanna
0
15
30
60
Kilometers

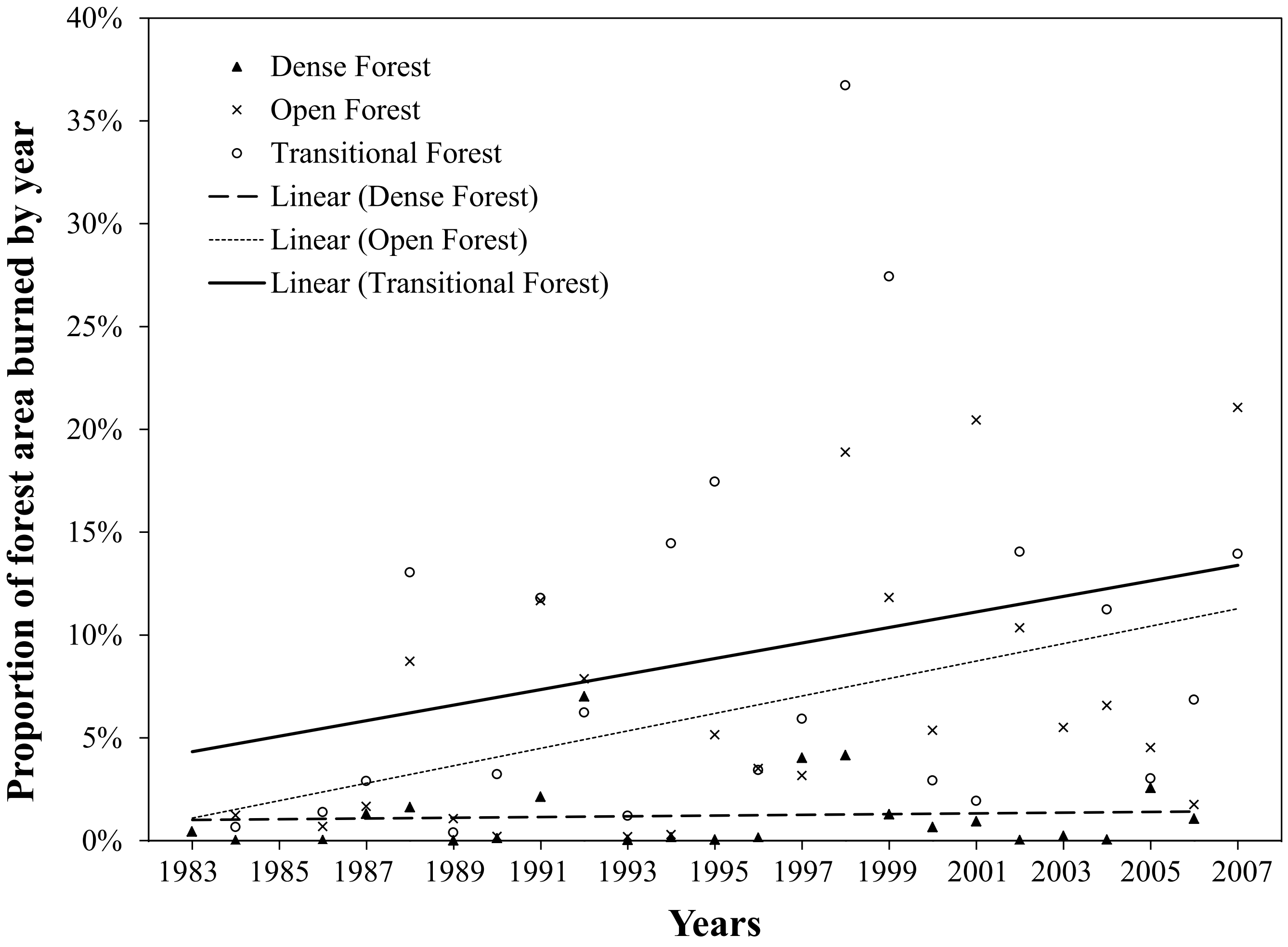
40%
35%
30%
25%
20%
15%
10%
5%
0%
Proportion of forest area burned by year
Dense Forest
Open Forest
Transitional Forest
Linear (Dense Forest)
Linear (Open Forest)
Linear (Transitional Forest)
1983
1985
1987
1989
1991
1993
1995
1997
1999
2001
2003
2005
2007
Years

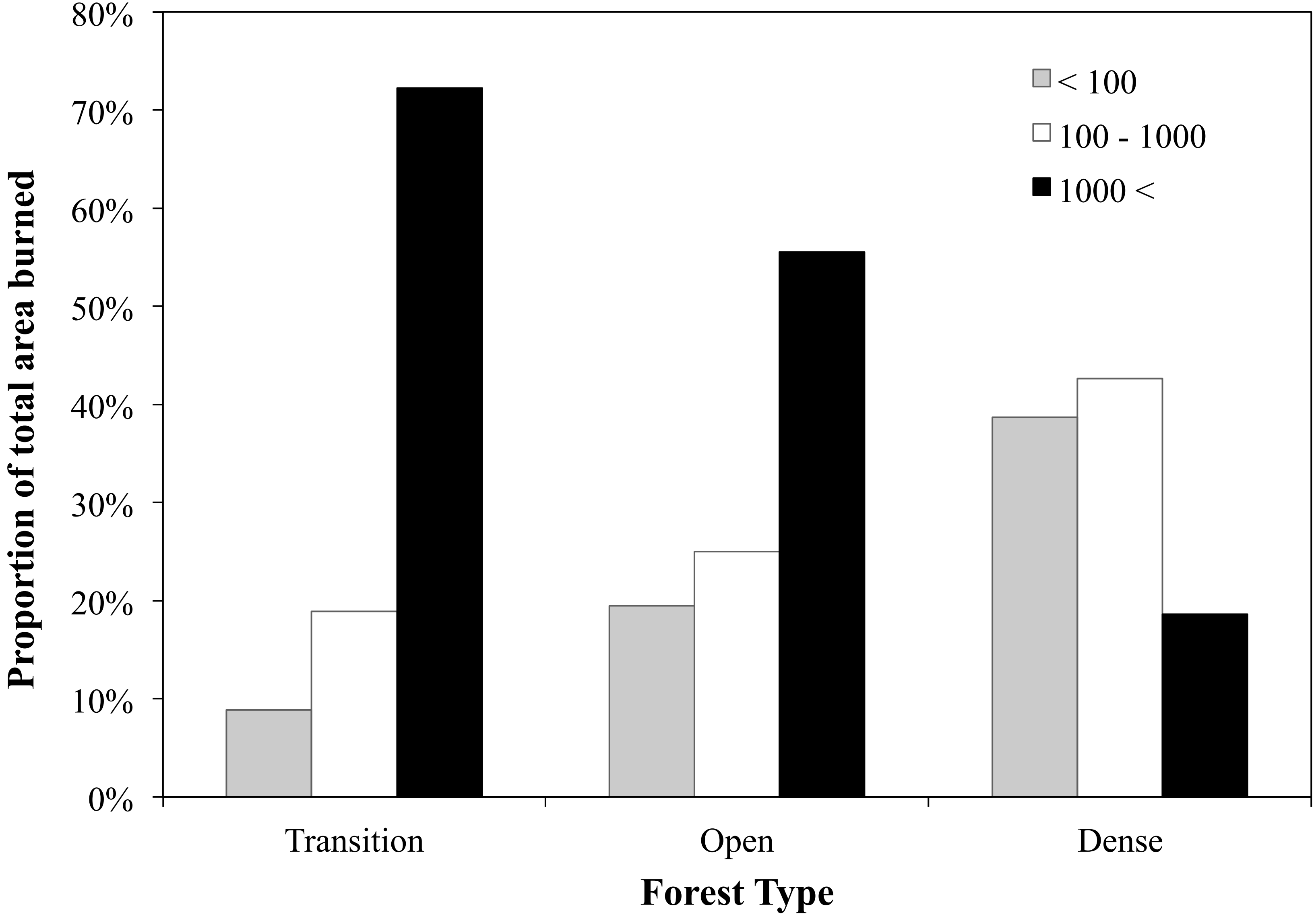
80%
70%
60%
50%
40%
30%
20%
10%
0%
Proportion of total area burned
< 100
100 - 1000
1000 <
Transition
Open
Dense
Forest Type

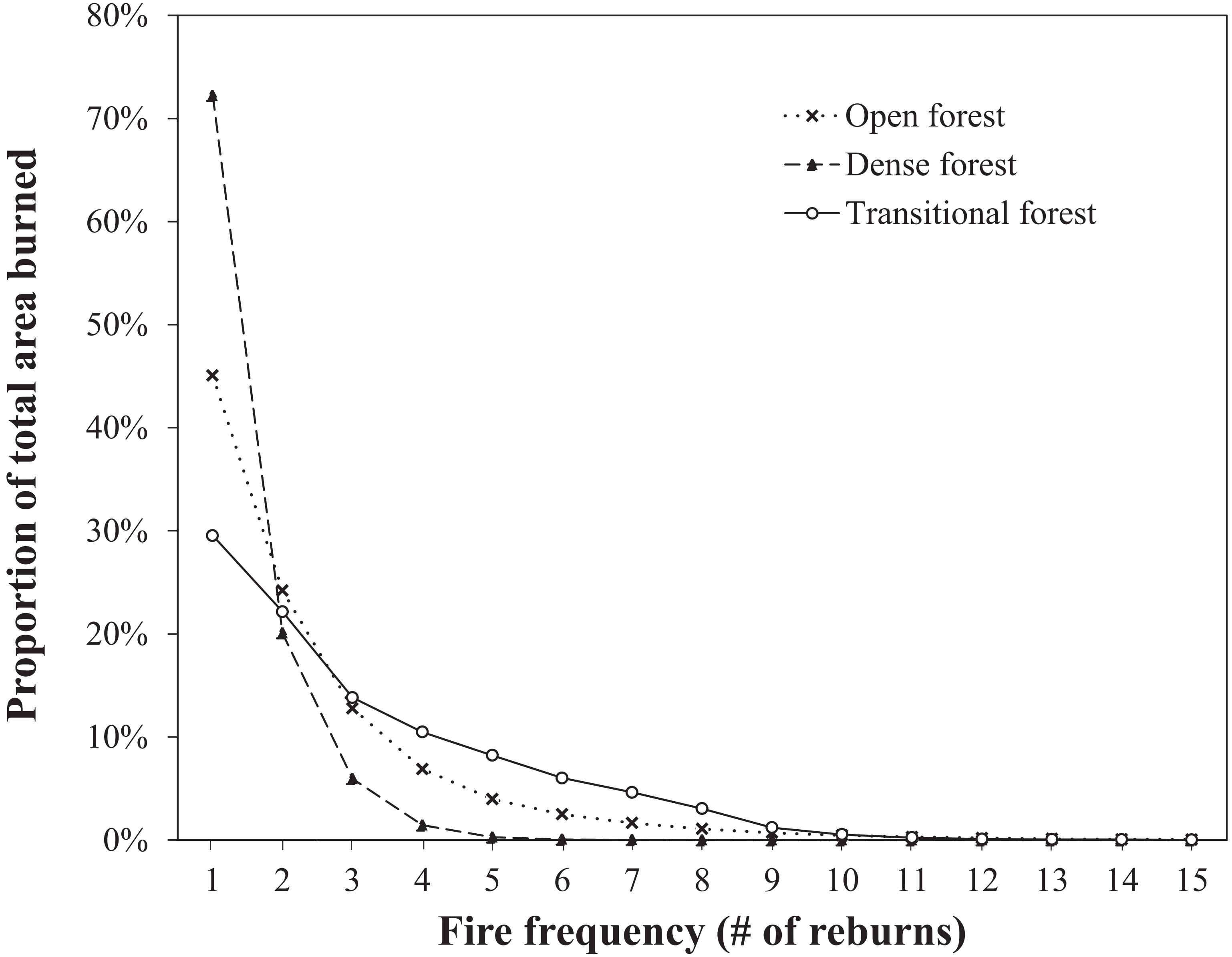

80%
70%
60%
50%
40%
30%
20%
10%
0%
Proportion of total area burned
Open forest
Dense forest
Transitional forest
1
2
3
4
5
6
7
8
9
10
11
12
13
14
15
Fire frequency (# of reburns)

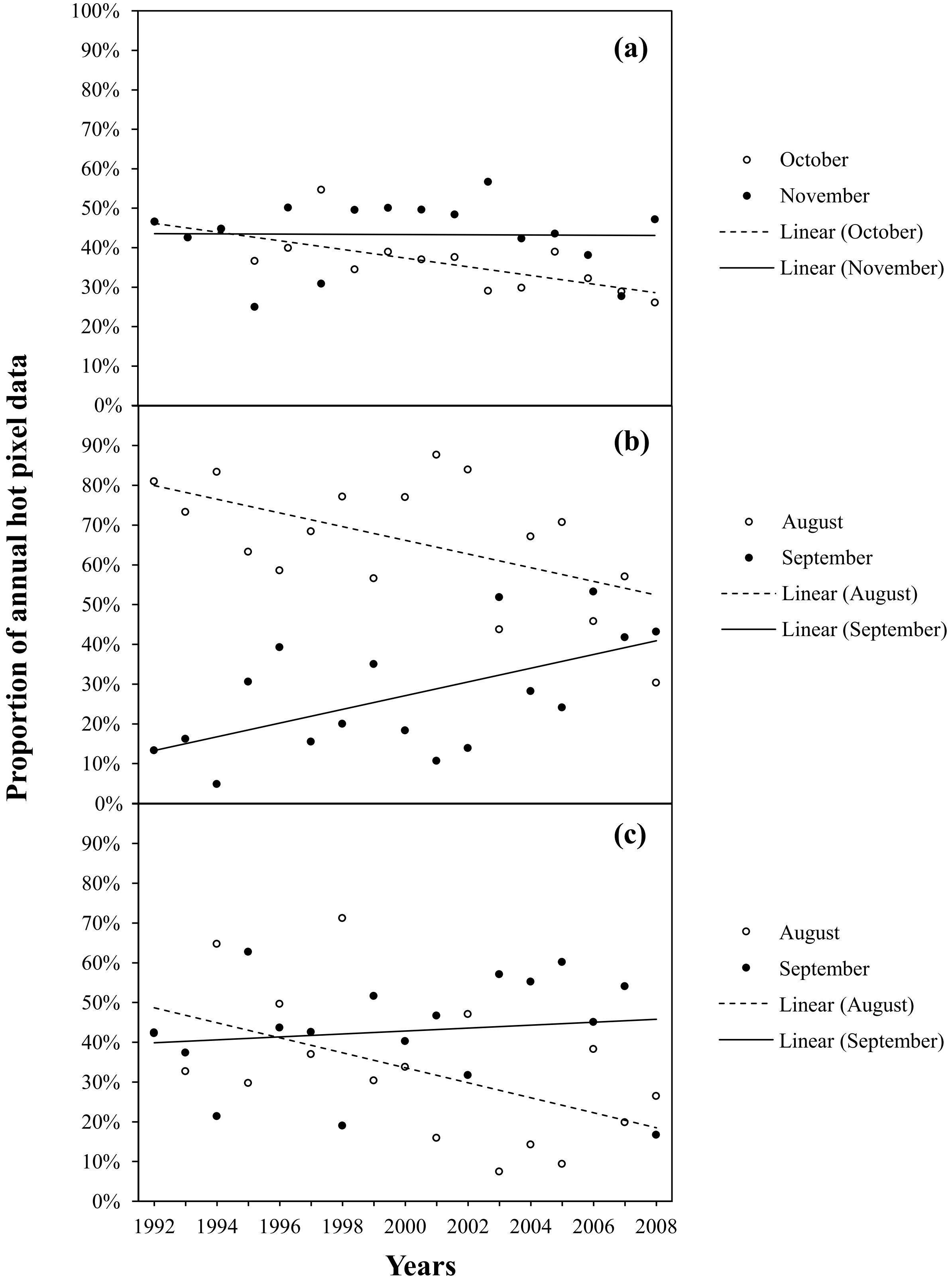

Proportion of annual hot pixel data
(a)
(b)
(c)
100%
90%
80%
70%
60%
50%
40%
30%
20%
10%
0%
1992
1994
1996
1998
2000
2002
2004
2006
2008
Years
October
November
Linear (October)
Linear (November)
August
September
Linear (August)
Linear (September)
August
September
Linear (August)
Linear (September)

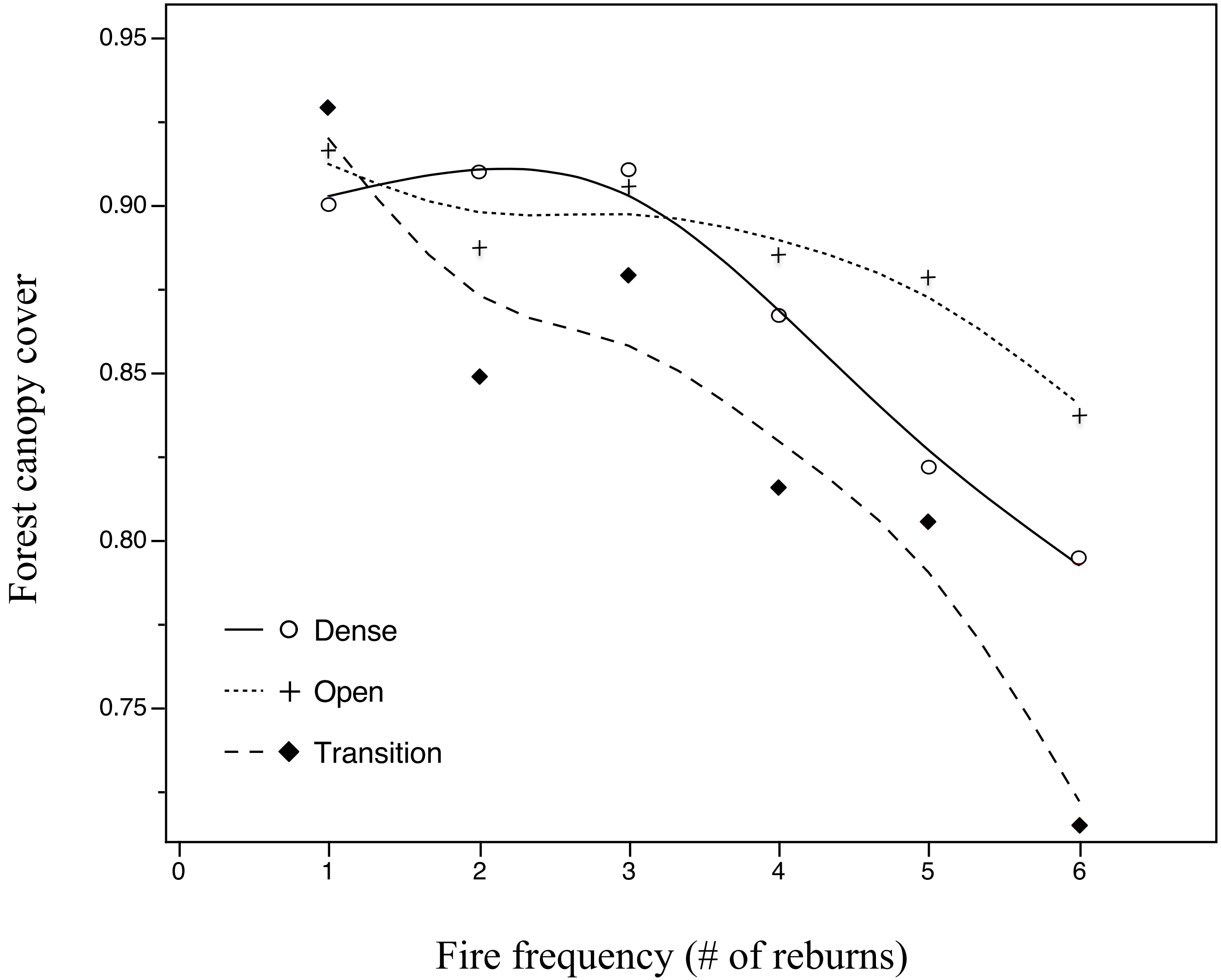
Forest canopy cover
0.95
0.90
0.85
0.80
0.75
0
1
2
3
4
5
6
Fire frequency (# of reburns)
Dense
Open
Transition

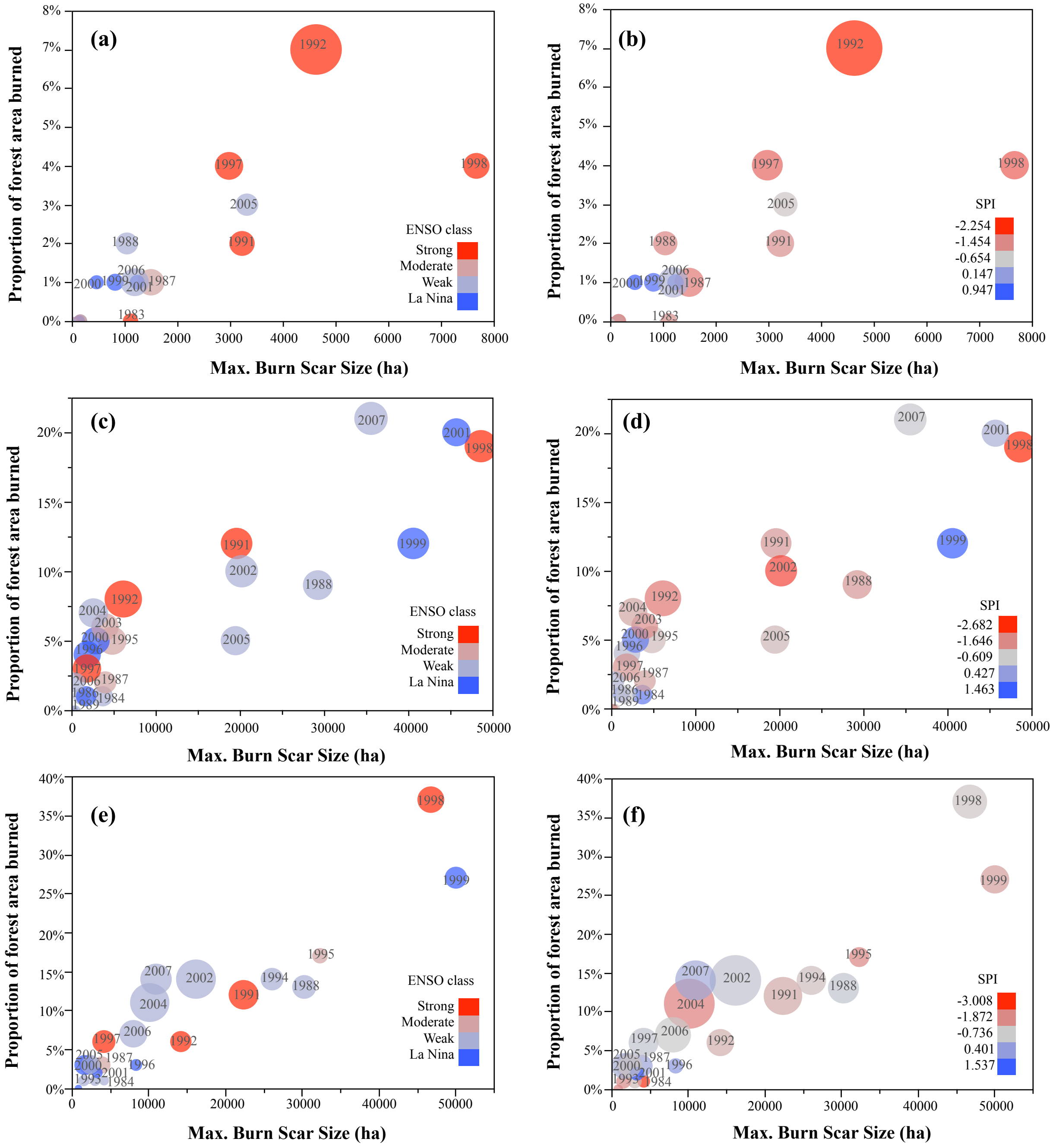
(a)
(b)
(c)
(d)
(e)
(f)
Proportion of forest area burned
Max. Burn Scar Size (ha)
0%
1%
2%
3%
4%
5%
6%
7%
8%
0
1000
2000
3000
4000
5000
6000
7000
8000
1992
1997
1998
2005
1988
1991
2006
2000
1999
2001
1987
1983
ENSO class
Strong
Moderate
Weak
La Nina
SPI
-2.254
-1.454
-0.654
0.147
0.947
10%
15%
20%
10000
20000
30000
40000
50000
2007
2002
2004
2003
1995
1996
1986
1984
1989
-2.682
-1.646
-0.609
0.427
1.463
25%
30%
35%
40%
1994
1993
-3.008
-1.872
-0.736
0.401
1.537